Luminescence processes at chromium in GaAs

B. Deveaud, G. Picoli, and B. Lambert
Centre National d'Etudes des Télécommunications, LAB/ICM-22301 Lannion Cedex, France

G. Martinez
Service National des Champs Intenses, CNRS, LP 5201, 25 Avenue des Martyrs, 38042 Grenoble Cedex, France
(Received 29 September 1983)

In GaAs:Cr, the Cr^{2+} internal luminescence is not observed when excited with above-gap light, because the ^5E state of Cr^{2+} is above the conduction-band minimum. We report here on experiments which allow one to observe this luminescence: luminescence in $Ga_{x-1}Al_xAs$:Cr, luminescence in GaAs under hydrostatic pressure, or luminescence in GaAs excited with a yttrium-aluminum-garnet:neodymium laser at 1.32 μm (0.9 eV). The zero-phonon line of that luminescence is observed for the first time and corresponds well to the absorption line. It is shown that in any case the radiative transitions are the results of a balance between the internal transition (A) and the band-to-level transition (B). Photoluminescence excitation spectra of the various luminescence bands involving Cr^{2+} are reported, and they allow one to confirm the previously proposed schemes. A model is developed, in terms of one-electron orbitals, to explain the characteristics of the photoluminescence excitation processes for Cr^{2+} as well as for other transition-metal ions in III-V materials. Internal luminescence at Cr^{2+} is shown to be mainly excited through the capture of electron-hole pairs by Cr^{2+} centers. This model allows one to propose some kind of Auger effect to explain the Cr^{2+}-related photoconductivity in III-V compounds. Finally, various band-shape calculations are performed that lead to the conclusion that spin-orbit effects on the band shape are negligible and that the main effect is due to a quadratic Jahn-Teller effect in the ^5E excited state.

INTRODUCTION

Technological applications, such as field-effect transistors (FET) or integrated circuits need the use of semi-insulating GaAs substrates. Such substrates have been realized by chromium doping. Resistivities up to 10^9 Ω/cm are obtained in this way. However, a lot of difficulties have occurred: exodiffusion of chromium during thermal processing leading to n-type conversion,[1,2] diffusion of chromium into epitaxies grown on chromium-doped substrates,[3] etc. Owing to these problems and to the importance of the possible applications, a lot of studies have been devoted to chromium in GaAs.

A coherent picture has been obtained for chromium (see, for example, Ref. 4). Chromium gives rise to an acceptor level (Cr^{2+}/Cr^{3+}) near midgap, and that level explains the semi-insulating properties of GaAs:Cr for the case when the chromium concentration exceeds the background donor level. This level is the one that has a technological importance. However, chromium on a gallium site (isolated) gives rise to other levels: the Cr^{+}/Cr^{2+} level which other workers have positioned 60 meV above the conduction-band minimum,[5] and the Cr^{3+}/Cr^{4+} level, a donor level of chromium, located about 300 meV above the valence band.[6,7] Furthermore, chromium can form complexes; the first that has been observed gives rise to the well-known 0.839-eV luminescence line.[8,9,4] The most probable associations for that complex are Cr^{2+}-O or Cr^{2+}-V_{As} (Refs. 10 and 11) (V_{As} means arsenic vacancy). One other complex has recently been observed to give a luminescence line at 0.844 eV.[12] The situation for chromium is thus quite the same as that observed for Ni in GaAs and GaP (Ref. 13) and also for Co in GaAs (Ref. 14): The transition-metal ions in III-V compounds may quite easily form associates with other impurities.

In the present paper we shall deal with the luminescence properties of isolated chromium related either to the Cr^{2+}/Cr^{3+} level or to the Cr^{2+} charge state. This charge state and that level have been characterized by various methods. For example, EPR,[15–18] photoluminescence (PL),[19,20] deep-level transient spectroscopy (DLTS),[21] absorption,[22,23] deep-level optical spectroscopy (DLOS),[20] photoluminescence excitation (PLE), etc.[20] A configuration coordinate diagram (see Fig. 1) has been proposed in Ref. 19 to explain the luminescence properties yttrium-aluminum-garnet (YAG) laser excitation; this model has been confirmed by PLE and DLOS experiments in Ref. 20. A Cr^{2+} ion has four d electrons ($3d^4$); the ^5D ground-state degeneracy of the free ion is split by the tetrahedral field of the crystal.[24] We thus obtain a $^5T_2$ ground state and a ^5E excited state. Both states can be subjected to Jahn-Teller distortions. The internal luminescence of Cr^{2+} corresponds to the transition between the ^5E and the $^5T_2$ states as observed in II-VI compounds both in absorption[24] and luminescence.[25–27]

Figure 1 explains why the internal transition of isolated Cr^{2+} is not observed: The ^{5}E excited state is above the conduction band minimum and the luminescence is very improbable. The degeneracy of the ^5E level with the conduction band has been further demonstrated by Eaves *et al.*[28] by photoconductivity measurements. On the contrary, for the trigonal chromium the ^5E excited state is

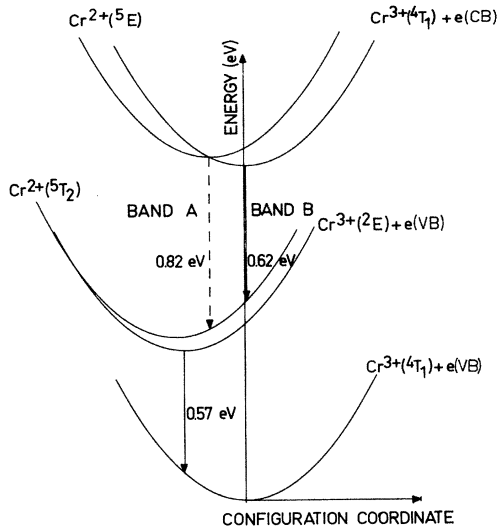

FIG. 1. Configuration coordinate diagram for the Cr^{2+}/Cr^{3+} system in GaAs. Only one coordinate is presented although several should be necessary, since the Cr^{3+} center is coupled to ϵ and τ_2 vibration modes, and the Cr^{2+} center to ϵ modes. The main features of the center can, however, be sketched on this diagram. Internal luminescence between the ^3E state and the $^5T_2$ state of Cr^{2+} is not possible because the ^5E state is above the conduction-band minimum.

below the conduction-band edge, and the 0.839-eV luminescence is then allowed.[4,29]

In previous work[29,30] we have shown that the internal luminescence of Cr^{2+} could be observed as soon as the ^5E level was brought below the conduction-band minimum. This is possible by two means: alloying GaAs with AlAs (Ref. 29) or applying an hydrostatic pressure to GaAs.[30] We detail here these first experimental results and complete them by PLE studies on degenerated GaAs:Cr. We also show that the internal transition of Cr^{2+} can be observed by using 1.32-μm excitation (0.9 eV) and observe the zero-phonon line (ZPL) of that transition for the first time. We shall show that luminescence in n-type GaAs:Cr samples can be described by the combination of two processes.

The internal luminescence of Cr^{2+}, process A:

$$Cr^{2+}(^5E)\rightarrow Cr(^5T_2)+h\nu\ ,$$

and the conduction band towards Cr^{3+} transition, process B:

$$Cr^{3+}+[e(CB)]\rightarrow Cr^{2+}(^5T_2)+h\nu\ ,$$

where e(CB) represents the electron in the conduction band. The experiments that we have performed cannot differentiate a band-to-level transition from a donor-to-level transition. Both of them probably occur.

All these experiments confirm the models that were proposed in Refs. 4, 19, 25, and 30. They explain the variation of the band shape under hydrostatic pressure[30] and allow one to propose a model, in terms of one-electron orbitals, for the recombination processes of transition-metal ions.

The present paper is organized as follows. We first give the experimental results concerning the isolated Cr^{2+} ($Ga_{1-x}Al_xAs$:Cr experiments, hydrostatic pressure experiments, and luminescence in GaAs:Cr excited by YAG:Nd laser at 1.32 μm (0.9 eV). In Sec. II we discuss these experimental results. We initially show how the shape of the internal luminescence is obtained. Then a discussion of luminescence processes of transition-metal ions in terms of one-electron orbitals is presented. In the last section calculations of the band shape will be given.

I. EXPERIMENTS

A. Cr^{2+} luminescence in $Ga_{1-x}Al_xAs$

Cr-doped $Ga_{1-x}Al_xAs$ samples have been obtained by diffusion in $Ga_{1-x}Al_xAs$ epilayers grown on n-type GaAs. The 20-μm-thick epilayers of Al concentration ranging between 11 at.% and 36 at.% were kindly furnished by Mr. Varon (la Radiotechnique Compelec, Caen) and were diffused at 900 °C for 15 min. Before diffusion, the samples are coated with sputtered Si_3N_4. Luminescence is excited by the 5145-Å line of an argon laser, detected with a PbS cell and analyzed by a 1-m monochromator. A typical result is shown in Fig. 2. This band, peaking at 0.73 eV, is missing before chromium diffusion and very strong after such a diffusion. However, its intensity decreases quickly as the Al concentration increases from 11 at.% to 36 at.% (a factor of 100 is observed between 11 and 36 at.%). The band does not show any zero-phonon line, although a very smooth structure is detectable in the spectra of the 11-at.% and 20-at.% Al samples. The whole band has a characteristic shape: a two humped band.

This luminescence band has been interpreted in Ref. 29 as the internal transition of Cr^{2+}. Following the work of Kocot *et al.*,[31] the ^5E level is found to be lower than the conduction-band minimum for aluminum concentrations greater than about 10 at.%. It is therefore easy to understand why the Cr^{2+} luminescence is so strong in the 11-

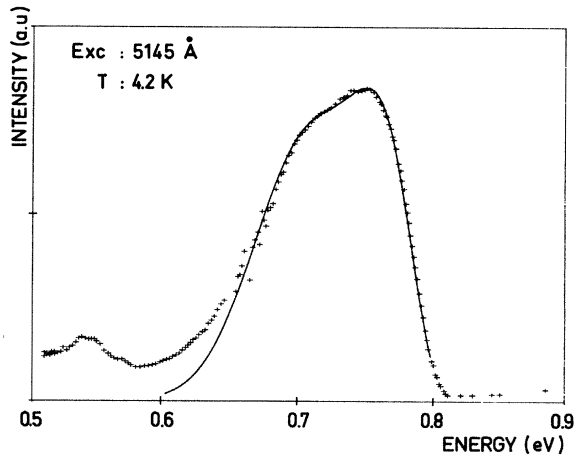

FIG. 2. Cr^{2+} internal luminescence in $Ga_{1-x}Al_xAs$:Cr ($x=0.24$) excited with an argon laser. +, experimental points; the solid line is the approximate band shape (two gaussian band) that will be used in the different band-shape fitting procedures.

at. % Al sample: The ^5E level is almost in resonance with the conduction-band minimum and the capture of photoexcited carriers is very efficient. In agreement with the work of Kocot *et al.*,[31] the luminescence band is observed to shift slightly towards low energies as x increases. The half width of the band does not change within experimental error.

The intensity variation between $x=11$ at. % and 36 at. % of aluminum can be due to variation in the capture cross section of photoexcited carriers at Cr^{2+} centers, but it might also be due to differences in the chromium content. Chromium concentrations after diffusion at 900 °C are below the detection limit of secondary ion emission spectroscopy (SIMS), 10^{15} cm^{-3}, and cannot be measured. It should also be noted that we are dealing with very inhomogeneous chromium distributions, since no etching has been performed after diffusion.

Cr^{2+} internal luminescence in ZnS has been observed by Grebe and Schulz.[26] They found an intense zero-phonon line at 4 K. In $Ga_{1-x}Al_xAs$, such a ZPL is not observed at the same temperature. Two reasons can be invoked for this.

(i) Residual strains at Cr^{2+} induced by the diffusion in the $Ga_{1-x}Al_xAs$ layers. As already mentioned the surface cannot be etched after diffusion due to the small thickness of the layer.

(ii) Inhomogeneity of the crystal field around the Cr^{2+} centers, is also possible. The Al atoms being randomly distributed in the lattice, a chromium ion on a gallium site may have different neighborhoods: 0,1,2... Al atoms as second neighbor.

PLE spectra have been performed on $Ga_{1-x}Al_xAs$:Cr. The spectra cannot be taken with a conventional system, since several bands are present when the exciting light has an energy lower than the gap of $Ga_{1-x}Al_xAs$. We have thus recorded luminescence spectra by using a dye laser and the spectra at each excitation wavelength are then deconvoluted (see Fig. 3). For example, in $Ga_{1-x}Al_xAs$:Cr with $x=11$ at. % two bands appear: the band corresponding to Cr internal transition, peaking at about 0.76 eV, and a band peaking at 0.66 eV which is 140 meV wide. The true PLE spectrum is then taken point by point by measuring the respective height of the two bands, as reported, for example, in Fig. 3. The same procedure has been applied to $Ga_{1-x}Al_xAs$:Cr $x=20$ at. %, where the second band appears to be centered at about 0.68 eV. The PLE spectra cannot be obtained for larger Al contents, both due to the luminescence efficiency and to the dye that we used.

The 0.66-eV band in $Ga_{1-x}Al_xAs$:Cr, $x=11$ at. % and the 0.68-eV band in $Ga_{1-x}Al_xAs$:Cr, $x=20$ at. % are interpreted as the transitions

$$Cr^{3+}+e(CB)\rightarrow Cr^{2+}+h\nu$$

(transition *B*).

The change in position of that band with x is coherent with such an attribution [the corresponding band in GaAs:Cr is at 0.62 eV (Refs. 19 and 20)]. In these two cases, the PLE spectrum shows a dramatic increase of the band *A* intensity at the band edge. In the case of $Ga_{1-x}Al_xAs$, $x=11$ at. %, a factor of 1000 is observed.

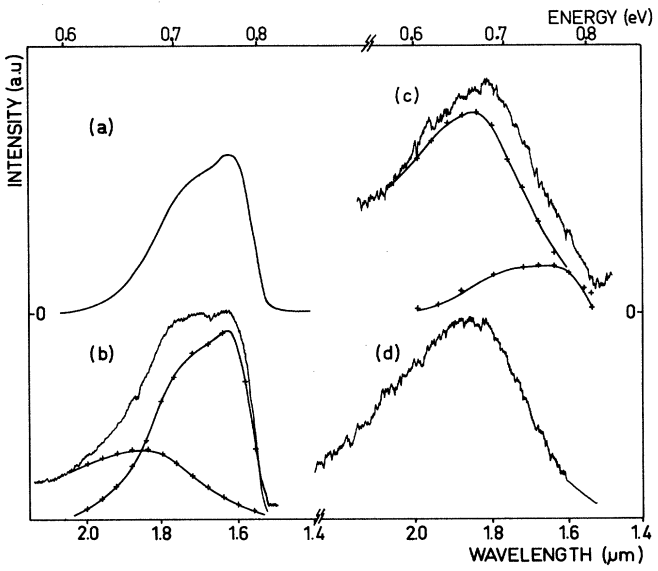

FIG. 3. Luminescence of $Ga_{1-x}Al_xAs$:Cr ($x=0.11$) using various excitation wavelengths. The excitation is performed with a dye laser: (a) 0.708 μm, above-gap light; (b) 0.720 μm; (c) 0.732 μm; (d) 0.760 μm. The band shape of (d) is subtracted from all spectra (by adjusting its height at 2 μm) and gives in any case the band shape of (a) (band *A*). Band *A* intensity is divided by a factor of 1000—when exciting below the gap energy.

Such a variation cannot be explained only by the change in the absorption coefficient of the sample since the band *B* does not show this type of variation. The explanation of this increase will be given in the discussion.

B. Cr^{2+} luminescence in GaAs under hydrostatic pressure

Hydrostatic pressure experiments have been reported in Ref. 30. Different samples are used, doped with Cr either during growth or by diffusion, with a concentration close to 10^{17} cm^{-3}. The pressure is obtained by compression of helium gas in a cell immersed in a liquid-nitrogen bath, a procedure that preserves the hydrostaticity of the stress. The luminescence is excited with an argon laser (5145-Å line), and detected through the sample by a cooled PbS cell. The results are corrected for the system transfer function.

Luminescence spectra under hydrostatic pressure are very similar for both types of samples and are perfectly reversible. A typical result is shown in Fig. 4. The luminescence increases linearly up to about 8 kbar and then the variation is more rapid. The shape of the band also changes, together with the activation of the luminescence. The band has almost the same shape and the same width (at 77 K) as the corresponding band in $Ga_{1-x}Al_xAs$.

This band is interpreted as an internal transition of Cr^{2+}.[30] The difference in energy, as compared to $Ga_{1-x}Al_xAs$, is due to the fact that the crystal-field splitting increases with hydrostatic pressure (as measured also by absorption,[23]) whereas it diminishes slightly in

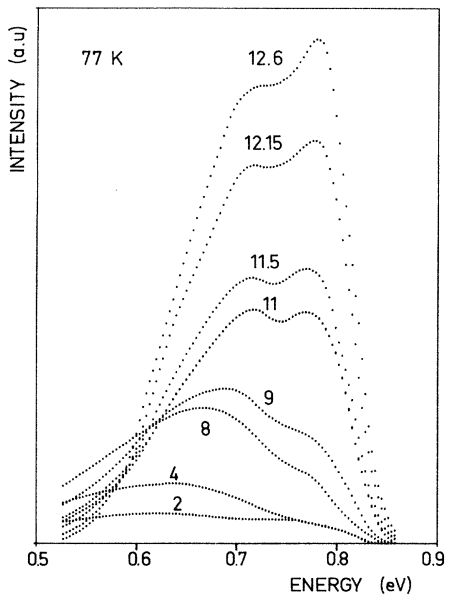

FIG. 4. Luminescence of GaAs:Cr under hydrostatic pressure. The sample temperature is 77 K. The respective pressures are indicated (in kbar).

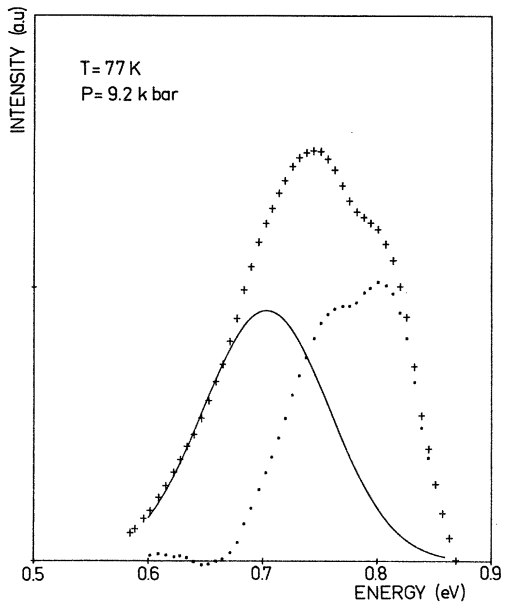

FIG. 5. Deconvolution of the luminescence in GaAs:Cr under hydrostatic pressure (9.2 kbar) (crosses) in two bands. Band *B*: a Gaussian band peaking at $0.62\pm0.009\times9.2=0.703$ eV and 0.130 eV width, the intensity of which is adjusted to fit the low-energy part of the band (solid line). 0.62 eV is the position of band *B* at 1 bar, 9 meV/kbar is the variation of the energy distance of the Cr^{2+} level to the conduction band, and so band *B* is expected to be centered at 0.703 eV at 9.2 kbar. Band *A*: The shape is obtained at high pressure by subtracting band *B* from the observed spectrum (dotted line).

$Ga_{1-x}Al_xAs$ as a function of Al concentration. The total luminescence shape is now interpreted (as in $Ga_{1-x}Al_xAs$) as due to the superimposition of two competing processes. The two bands are the Cr^{2+} internal transition band (transition *A*) and the band *B* corresponding to the transition:

$$Cr^{3+}+e(CB)\rightarrow Cr^{2+}$$

(transition *B*), which is at 0.62 eV in GaAs at 1 bar and moves up to 0.73 eV at 12.6 kbar.

So we have fitted our results assuming a Gaussian band for a transition peaking at 0.62 eV at 1 bar and moving at a rate of 9 meV/kbar (pressure coefficient of the $^5T_2$ ground state of Cr^{2+} with respect to the conduction band[22]). A constant width of 130 meV has been assumed in accordance with the negligible variation of the lattice relaxation as a function of the pressure.[23] This band is subtracted from the experimental spectra, and results are shown in Fig. 5. The high-energy contribution has the characteristic shape of the internal transition of Cr^{2+}, at least above 9 kbar, and the energy of the maximum moves at a rate of 1.7 ± 0.2 meV/kbar in very good agreement with the coefficient (1.6 meV/kbar) found in absorption.[23] This is due to the increase of the crystal-field splitting Δ as a function of the pressure whereas, as already noticed, Δ decreases with the Al content. The extrapolation to 1 bar gives an energy of 0.788 ± 0.002 eV for this maximum. Below 9 kbar the fit is not very precise but the shape of the spectrum seems to change, the high-energy extremum being more affected than the low-energy one when the ^5E level merges into the conduction band. The integrated intensity of both contributions is plotted in Fig. 6.

Below 6 kbar the intensity of the *B* transition increases linearly, a point which reflects a well-known property of the increase of spontaneous emission rate at a function of the energy between initial and final states.[32] Above that

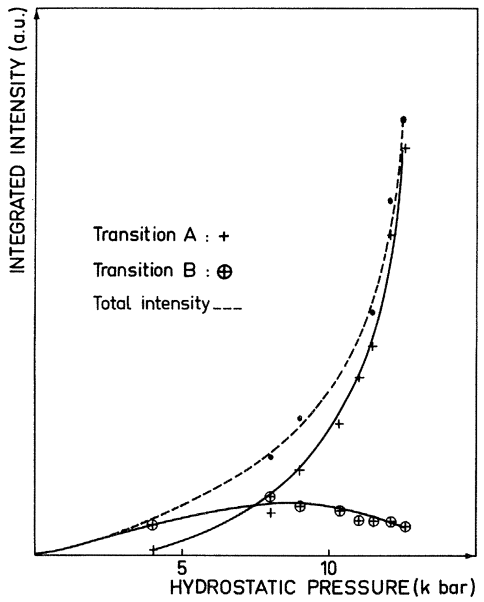

FIG. 6. Integrated intensity of bands *A* and *B* as a function of hydrostatic pressure. The band intensities are obtained by the fitting procedure exposed in Fig. 5. Band *B* shows a smooth increase up to 8 kbar and then diminishes. Band *A* is very weak up to 8 kbar and then rises very rapidly. Total integrated intensity is also plotted.

pressure process A begins to compete with process B and the lifetime τ of photoexcited carriers can be written as

$$\frac{1}{\tau}=\frac{1}{\tau_A}+\frac{1}{\tau_B}+\frac{1}{\tau_{NR}},$$

where τ_A and τ_B are the radiative lifetime of corresponding processes; the nonradiative lifetime τ_{NR} can be assumed constant as a function of the pressure since this does not affect the phonons much. As soon as process A starts to be energetically favored, process B saturates (between 7 and 8 kbar) and then decreases. Notice that the total intensity does not vary linearly with pressure, which clearly shows that the quantum efficiency of process A is much higher than that of process B.

C. Cr^{2+} internal luminescence in GaAs

In the two preceding sections, we have shown that the Cr^{2+} luminescence is seen under band-to-band excitation only when the ^5E state is no longer degenerated with the conduction band. However, this law holds for thermalized photogenerated carriers and the question arises if under specific conditions it would be possible to observe process A even for a resonant ^5E level. For this study, we have used the same chromium-diffused samples as for hydrostatic pressure measurements[30] or absorption studies.[22,23] The free-carrier concentration in the samples is given in Ref. 22; some of them have a carrier concentration in the $(10^{17}-10^{18})$-cm^{-3} range.

Cr^{2+} internal transition can be observed when using an internal excitation. This excitation is the most efficient at 0.9 eV (1.3 μm) so that a 1.32-μm YAG:Nd laser has been used (see PLE spectrum of Fig. 9). The obtained spectrum is displayed in Fig. 7. The high-energy part is quite complicated but can be resumed as follows: a weak contribution of the 0.839- and 0.844-eV lines that will be discussed elsewhere[12] and a principal contribution beginning at 0.820 eV. The ZPL at 0.820 eV can be resolved. It is very weak compared to the whole luminescence band (as in absorption). Three lines are observed at 0.8205 eV (6619 cm^{-1}), 0.8197 eV (6612.5 cm^{-1}), and 0.8194 eV (6610.3 cm^{-1}). Their intensities are, respectively, proportional to 2,2,1 (see Fig. 8). These lines are attributed to the Cr^{2+} internal transition. The corresponding lines in absorption have been resolved with a better accuracy;[33,34] the detailed interpretation is given by Abhvani *et al.*[33] Seven lines labeled $X_1,X_2,X_3,Y_1,Y_2,Z_1,Z_2$ are observed; their position and respective oscillator strengths are consistent with a $^5E\rightarrow{}^5T_2$ transition in a Cr^{2+} center.

In our case, the resolution is not sufficient to observe seven lines. We only observe three lines as expected if the slit width is larger than K (0.06 meV, 0.5 cm^{-1}; K is the spin-spin coupling constant in the ^5E excited state[24]). The same three lines were observed by Clerjaud *et al.*[35] They correspond to, respectively, $X_1+X_2+X_3$, Y_1+Y_2, Z_1+Z_2. The predicted splittings in that case are 6.5 and 2 cm^{-1}; we observed 6.5 and 1.8 cm^{-1}. The spectra are recorded at 4.2 K. Since the overall splitting of the initial state for luminescence (^5E) is 0.24 meV (2 cm^{-1}), all five levels can be assumed to be equally populated and the predicted intensities are directly given by the oscillator strengths[33]

$$X_1+X_2+X_3\ ,\quad 0.5+1+0.5=2\ ,$$
$$Y_1+Y_2\ ,\quad 0.5+1.5=2\ ,$$
$$Z_1+Z_2\ ,\quad 0.5+0.5=1\ .$$

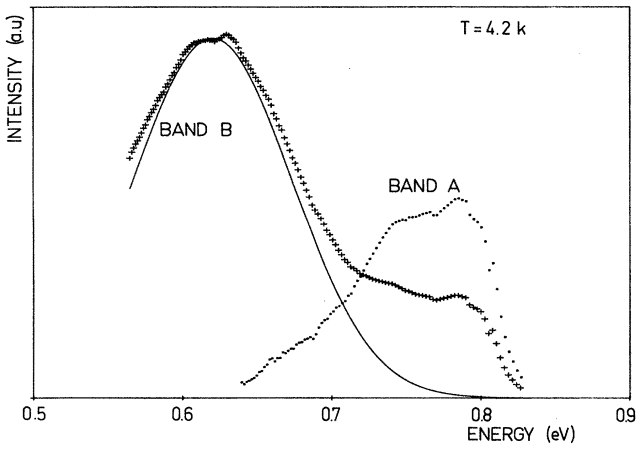

FIG. 7. Photoluminescence spectrum of GaAs:Te:Cr sample excited with a 1.32-μm (0.92-eV) YAG Laser. This luminescence shows a band centered at 0.62 eV (band B) and a high-energy part. When the high-energy part is obtained by subtraction (dots), it can be fitted by the $Ga_{1-x}Al_xAs$:Cr band shape.

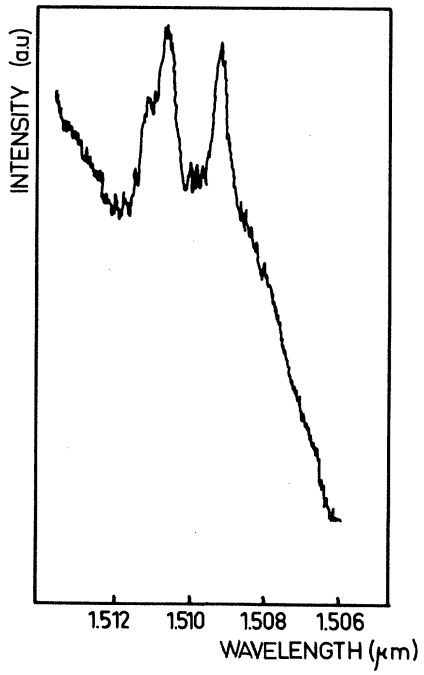

FIG. 8. ZPL appearing (with 1.32-μm YAG laser excitation) at 0.820 eV. Three components can be distinguished at 820.5 meV (6619 cm^{-1}), 819.7 meV (6612.5 cm^{-1}), and 819.4 meV (6610.3 cm^{-1}). The intensity ratios predicted by theory are 2, 2, and 1, respectively.

These predictions are in very good agreement with the observed intensities.

In conclusion, the 0.820-eV ZPL in luminescence can be unambiguously attributed to the Cr^{2+} (isolated) internal transition. The shape of the whole band obtained with 1.32-μm (0.9-eV) YAG laser excitation is displayed in Fig. 7.

That band is obviously constituted by a Gaussian part centered around 0.62 eV (band *B*) and a high-energy part. The shape of the high-energy part which is due to transition *A* can be obtained easily by subtraction. As can be seen in Fig. 7, the obtained band shape is very comparable to that of the corresponding transition in $Ga_{1-x}Al_xAs$ or in GaAs at high pressure, and peaks at 0.787 eV in good agreement with the extrapolated value obtained in Sec. I B. So, 1.32-μm (0.9-eV) excitation in GaAs can lead to Cr^{2+} internal excitation; this is true in semi-insulating material as well.

As shown by Eaves *et al.*[28] 0.9-eV excitation leads to photoconductivity; their interpretation was that when Cr^{2+} is brought into the ^5E excited state, one electron may escape and go into the conduction band, giving rise to the photocurrent. So, when the system is excited as ^5E, two processes are competing: direct radiative recombination leading to internal luminescence or transfer of one electron into the conduction band, subsequently giving rise to the luminescence process *B*. The respective intensities of the two bands depend on the relative lifetime of both processes, and also of the possible competing processes (radiative or nonradiative). As a matter of fact, the intensity ratio between bands *A* and *B* in GaAs:Cr under 1.32-μm excitation does vary from one sample to another.

PLE spectra of both bands can be recorded (by using only below-gap light). The PLE spectrum of band *A* is excited with a 60-W halogen filament lamp dispersed by a 0.25-m monochromator. Detection is made with a germanium detector through a 1-m monochromator which is set at 1.57 μm (0.8 eV). For band *B*, detection is made by using a PbS cell and a Ge filter: That is to say, that we integrate the luminescence below 0.69 eV. Both spectra are plotted in Fig. 9. Photoconductivity has been recorded on the same samples in the same conditions.

PLE spectrum of band *A* is mainly a Gaussian band at 0.9 eV. This band closely corresponds to the beginning of the absorption spectrum of Cr^{2+}, or of the photoconductivity spectrum. It shows the classical shape observed for Cr^{2+} internal transition in II-VI compounds.[24] The main difference between the PLE spectra of bands *A* and *B* is a tail appearing between 1 eV and the band edge. This tail is also observed on the photoconductivity spectrum and on the DLOS spectrum[20] and has been interpreted as due to the transitions from Cr^{2+} to higher extrema of the conduction band.[20]

As a summary, the PLE spectra that we have observed on bands *A* and *B* are coherent with the attributions of the bands. The internal transition *A* is only excited by internal absorption. The band-to-level transition *B* can also be excited by Cr^{2+} towards conduction-band photoionization absorption.

On the same samples, other luminescence lines are observed especially when using above gap light: The 0.839-eV line that is attributed to a Cr^{2+}-*X* (unknown defect) center,[4,8,9,11,36–45] and also a new ZPL line at 0.844 eV that is interpreted as an internal transition to a Cr^{2+}-Te complex. Complete results will be presented in a forthcoming paper.[12]

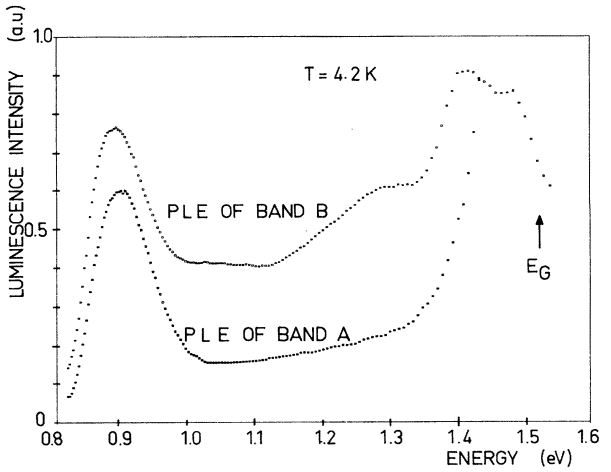

FIG. 9. Photoluminescence excitation spectra of GaAs:Cr:Te. The lower curve is obtained by setting the monochromator at 1.58 μm. The upper curve is the PLE obtained by using a PbS cell and a Ge filter (integrating energies below 0.69 eV).

II. DISCUSSION

A. Shape of the Cr^{2+} internal transition

Most of the spectra that we have obtained show simultaneously the Cr^{2+} internal transition (*A*) and the conduction band$\rightarrow Cr^{5+}$ level transition (*B*). Those two radiative transitions overlap and so it is necessary to separate them in order to have the true shape of the internal transition.

First we must stress that the picture obtained for transition *B* is very coherent. The maximum of the band is at 0.62 eV in GaAs. This corresponds very well to the level position relative to the conduction band (0.79 eV) minus the Franck-Condon shift 150 meV.[19,20,46] In $Ga_{1-x}Al_xAs$ ($x=11$ at. %), the transition is observed at 0.66 eV, which is about the expected position calculated from Kocot *et al.*[31] In GaAs under hydrostatic pressure, it moves at 9 meV/kbar, as could be expected from absorption experiments.[22,23]

Band *A* appears alone only in $Ga_{1-x}Al_xAs$. This is consistent with the observation made in GaAs under hydrostatic pressure: At 8 kbar, transitions *A* and *B* have the same intensity; at 12 kbar, the excited state of Cr^{2+} is about 35 meV lower and band *A* is 10 times more intense than band *B*. The pressure difference is equivalent to 2% or 3% more Al in GaAs. So it is probable that at 15 kbar, band *A* would appear alone in GaAs also.

But in $Ga_{1-x}Al_xAs$ samples, strains or inhomogeneities could be suspected to change the real shape of the band. We have thus been obliged to use several deconvolution procedures, for example as shown in Fig. 5, to try to ob-

tain the true shape of the Cr^{2+} internal emission band. The best try is shown in Fig. 7, where the band A appears, under 1.32-μm YAG laser excitation, together with the 0.62-eV band. As the shape of the 0.62-eV band is well known, it can easily be subtracted from the spectrum to give the shape which is shown in Fig. 7 and agrees very well with that observed in $Ga_{1-x}Al_xAs$:Cr (see Fig. 2).

B. Excitation process of the internal transition

The process of luminescence itself has been discussed by few authors.[47–49] The most advanced models were presented by Robbins and Dean.[47,49] However, such models do not explain all characteristics of the recombination at transition-metal centers. In order to explain the exact process, it is interesting to consider the one-electron schemes as presented by Hemstreet *et al.*[50] or by De Leo *et al.*[51]

The case of Cr^{2+} is presented in Fig. 10. The four d electrons of Cr^{2+} are distributed on e and t_2 orbitals: Two electrons on an e orbital and two on a t_2 orbital give rise to the $^5T_2$ ground state of Cr^{2+}. The ^5E excited state corresponds to one e electron and three t_2 electrons. The internal luminescence corresponds to the transfer of one electron from a t_2 orbital to an e orbital. In the same description, the $^4T_1$ ground state of Cr^{3+} is obtained with two electrons on an e orbital and one on a t_2 orbital.

We do not present the results of any single-particle calculation but simply use single-particle schemes. As shown by De Leo *et al.*,[51] the energy position of the Cr level in the band gap cannot be obtained directly on such a scheme. The level position relative to the conduction-band edge [$E(-/O)$ in Ref. 51] is the difference of the total energy of the electrons of the two configurations:

$$Cr^{2+}=(de)^2(dt_2)^2(3a_1)^0$$

and

$$Cr^{3+}+e(CB)=(de)^2(dt_2)^1(3a_1)^1\ ,$$

including the many-electron effects and lattice relaxation. The change in the different terms that are involved in $E(-/O)$ is represented by the shift of the e and t_2 orbitals. Therefore $E(-/O)$ should be obtained by summing the energy of each electron as indicated ($\uparrow$) and by calculating the difference between the respective configurations (see Fig. 10).

The question we wish to raise is one of how the ^5E excited state of Cr^{2+} is obtained. We of course consider a case where the luminescence is possible: $Ga_{1-x}Al_xAs$:Cr or GaAs:Cr under hydrostatic pressure (when the ^5E excited state is below the conduction-band edge). For the corresponding luminescence of Fe^{2+}, the well-known model is the capture of an electron by a Fe^{3+} center[52] (see also Fig. 11):

$$Fe^{3+}+e(CB)\rightarrow Fe^{2+}(^5T_2)\rightarrow \text{luminescence}\ .$$

The same model, in the case of Cr^{2+}, would lead one to add an electron on the Cr^{3+} ($^4T_1$) [see Fig. 10(h)]. This extra electron would seemingly go on a t_2 orbital and the resultant state is $^5T_2$ rather than ^5E. This would correspond to transition B, and not to transition A. Other

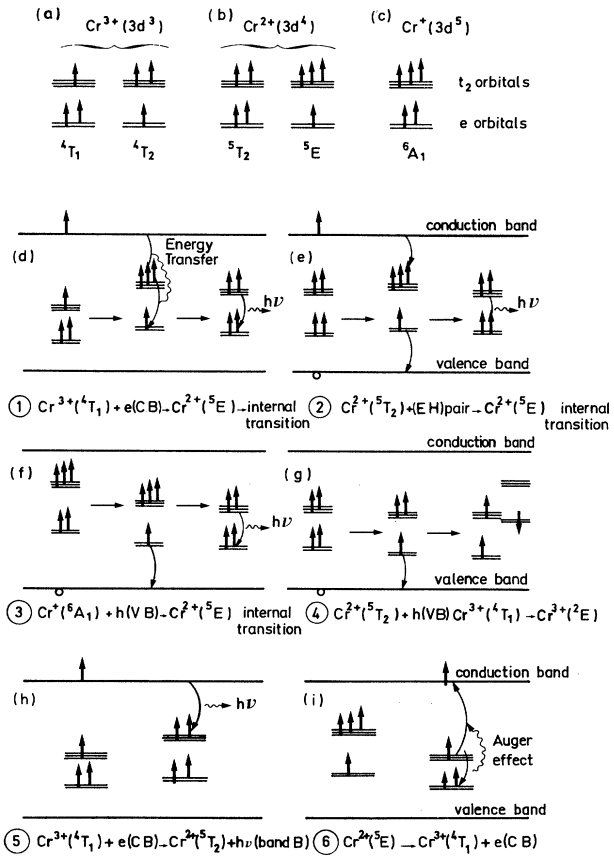

FIG. 10. One-electron schemes for Cr^{2+} luminescence excitation processes. (a), (b), (c): Description of the ground state and first excited state for Cr^{3+}, Cr^{2+}, and Cr^{+}, respectively. (d) Luminescence process 1; excitation of the internal luminescence is due to some energy-transfer process. In the absence of such a process, capture of an electron at a Cr^{3+} center would give rise to band B rather than band A [see (h)]. (e) Luminescence process 2; excitation of internal luminescence by capture of an electron-hole pair at a Cr^{2+} center. (f) Luminescence process 3; excitation of internal luminescence by capture of a hole at a Cr^{+} center. (g) Luminescence process 4; internal luminescence of Cr^{3+} can be obtained by capture of a hole by a Cr^{2+} center. (See Sec. II C.) (h) Luminescence process 5; capture of an electron on a Cr^{3+} center without an energy-transfer process would give rise to band B.

mechanisms must be assumed in order to create the ^5E luminescence initial state [see Figs. 10(d), 10(e), and 10(f)]:

$$Cr^{3+}+e(CB)\xrightarrow[\text{with "Auger" effect}]{}Cr^{2+}(^5E)\ ,$$

process (1).

The "Auger" effect is a kind of energy-transfer process that allows the energy gained by the conduction-band electron (when falling into the t_2 orbital) to be transferred to an e electron so that this second electron is promoted on a t_2 orbital. Such a process is the only one that would give the ^5E state when starting with Cr^{3+} and a photoexcited electron. This mechanism seems to be implied in the case of Cr^{2+}-X (0.839-eV line) by the optically-detected magnetic resonance (ODMR) experiments of Killoran *et al.*[53] It is favored in p-type materials since the luminescence in-

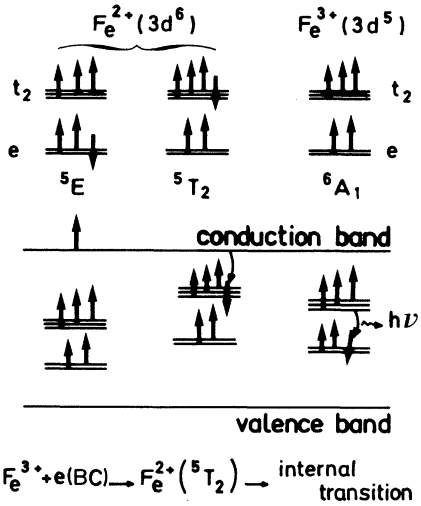

FIG. 11. One-electron schemes for Fe in III-V compounds showing the excitation process of the internal Fe^{2+} luminescence by capture of an electron on a Fe^{3+} center.

tensity depends on the number of Cr^{3+} centers, and so we may suppose that this process is not very efficient.

The second mechanism to be considered corresponds to the capture of an electron-hole pair or of an exciton at a Cr^{2+} ($^5T_2$) center. As shown in Fig. 10(e) this process, where an e electron is removed by the hole and where a t_2 electron is added, directly leads to a Cr^{2+} (^5E) state:

$$Cr^{2+}(^5T_2)+(\mathrm{EH})\text{ pair} \rightarrow Cr^{2+}(^5E)\ ,$$

process (2), where EH represents electron hole.

Beside the direct capture of an exciton at a Cr^{2+} center one can also imagine that an electron is captured first, then the center is negatively charged twice and may attract a hole. When the hole is captured, the system becomes Cr^{2+} (^5E). If a hole is captured first, for the internal luminescence of Cr^{2+} to occur, the excited Cr^{3+} center must capture an electron in a time shorter than the radiative lifetime of the excited state of Cr^{3+}.

In this case, the luminescence intensity would be proportional to the number of Cr^{2+} centers and thus favored in n-type material. Besides the direct mechanism of internal excitation in Cr^{2+} (performed by 1.3-μm YAG laser excitation) which obviously leads to the ^5E state by directly promoting an e electron to a t_2 orbital, there is one more possible mechanism:

$$Cr^{+}+\text{hole (VB)} \rightarrow Cr^{2+}(^5E)$$

(where VB represents valence band), Fig. 10(f), process (3). This mechanism is possible if the Cr^{+} level is below the conduction-band edge and if the material is sufficiently n type for chromium to be in the Cr^{+} charge state.

In order to choose the more efficient of these possible mechanisms, it is very interesting to come back to the PLE spectra. Indeed the great difference between processes (1) and (2) is that the latter is not activated below the gap whereas the activation cross section of the first one should correspond to the photoionization of Cr^{2+}. In GaAs, PLE results cannot be interpreted close to E_g as above gap excitation leads to transitions related to complexes (Cr^{2+}-X, 0.839-eV line, or Cr^{2+}-Te, 0.844-eV line[12]), but below 1.4 eV there is an obvious difference between PLE of bands A and B: Excitation of band A is only performed by internal excitation of Cr^{2+} around 0.9 eV (see Fig. 9). On the contrary, the PLE spectrum of band B is quite similar to the photoionization cross section σn^0 of Cr^{2+} as already shown by Nouailhat *et al.*[20]

PLE results on $Ga_{1-x}Al_xAs$ (see Sec. I A) show that band A (internal transition) cannot be excited by below-gap light, and that this transition is only efficiently excited when the incident light has an energy larger than the band gap E_g; transition A is only excited when electron-hole pairs are created. On the contrary, although weaker in $Ga_{1-x}Al_xAs$, band B is obtained with energies below the gap and its intensity does not change much when crossing E_g.

As Cr^{2+} internal transitions can be observed by above-gap excitation in SI GaAs under hydrostatic pressure (in this material, Cr^{+} centers cannot be filled with electrons when applying pressure), the third possible mechanism does not seem to be involved. PLE results on the Cr^{2+} internal transition thus imply that the luminescence process is related to the capture of an electron-hole pair on a Cr^{2+} center.

The model that we have developed can be confirmed by studying the PLE results for other transition-metal ions in III-V materials. Such spectra have been reported for Fe in GaAs, InP, and GaP (Refs. 54, 52, and 55), for Co in InP and GaAs,[56,14] and for Ni in GaP.[48]

As reported in Figs. 11 and 12, it can be seen that contrary to Cr^{3+}, the capture of an electron by a Fe^{3+} center or by a Co^{3+} center naturally leads to the Fe^{2+} or Co^{2+} excited state.[52–57,14] This is what is observed in the PLE spectra of these ions. The onset of excitation of Fe^{2+} in InP corresponds to the σ_n^0 onset as it does for Co^{2+} in InP.[56,57] σ_n^0 has not been measured for Fe^{2+} in GaAs or for Co^{2+} in GaAs. The onset of Fe^{2+} PLE in GaAs is at

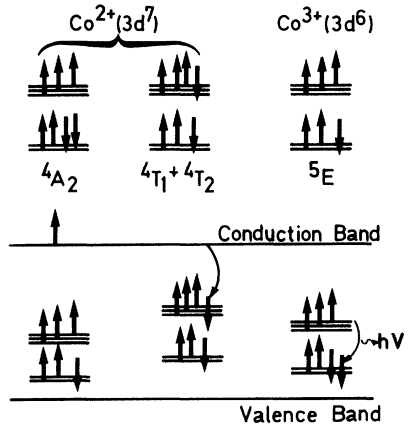

FIG. 12. One-electron schemes for Co in III-V compounds. Internal luminescence at Co^{2+} can be obtained by capture of an electron on Co^{3+} center.

1 eV, which is the approximate distance of the Fe^{2+} level from the conduction band. For Co in GaAs, no onset is observed[14] but since the Co level is very close to the valence band this is not really surprising.

So, the model that we have developed in terms of single-particle orbitals explains well how the excited state of transition-metal impurities is obtained and this enables us to explain some striking differences in the PLE spectra of those impurities.

C. Reinterpretation of the 0.57-eV band

Once this model is accepted, it is possible to return attention to the process occurring at Cr^{2+} centers. Luminescence is obtained by the capture of an electron-hole pair at the Cr^{2+}. In fact one might suppose that a hole is captured first (since the Cr^{2+} center carries a net negative charge) and that the electron is then captured very rapidly. If we apply the model we proposed in Ref. 19, capture of a hole at a Cr^{2+} center should give rise to the 0.57-eV luminescence band. However, a more careful look at the involved process of a one-electron scheme leads us rather to predict a Cr^{3+} internal transition [see Fig. 10(g)]:

$$Cr^{2+} + \text{hole(VB)} \rightarrow Cr^{3+}(^4T_2) \rightarrow Cr^{3+}(^4T_1) + h\nu$$

As can be seen in Fig. 10(g), capture of a hole at a Cr^{2+} center is expected to leave the system in an excited Cr^{3+} ($^4T_2$) configuration.

The Cr^{3+} internal transition is obtained if the electron is captured before the internal luminescence of Cr^{2+} takes place. So, our model would predict for the 0.57-eV luminescence an internal transition process.

This is coherent with two experimental facts that have not been successfully explained yet. The PLE spectrum of the 0.57-eV band[20] does not coincide with the photoionization absorption transition at Cr^{3+} centers. Furthermore, we have carried out very careful luminescence experiments under 1.06-μm excitation (1.17 eV) where the 0.57-eV band is observed: A very small (barely detectable) ZPL appears at 1.86 μm (0.666 eV). The fact that a ZPL appears, and that its position does not correspond to the thermal threshold for Cr^{3+} ionization [0.735 eV (Ref. 22)], are in conflict with the attribution of that band to a transition:

$$Cr^{2+} + \text{hole(VB)} \rightarrow Cr^{3+} + h\nu\ .$$

Our new interpretation would be that the 0.57-eV band is an internal transition to Cr^{3+}.

Many absorption experiments have been carried out in semi-insulating GaAs:Cr materials containing a large amount of Cr^{3+} centers, and no absorption beginning at 0.666 eV has been detected. If our interpretation of the luminescence is correct, we are therefore led to speculate that this transition is spin-forbidden though very weak in absorption. Crystal-field splittings for a d^3 ion at intermediate Dq suggest a possible $^2E \rightarrow {}^4T_2$ transition (see Fig. 6 of Ref. 57 for $Dq = 400\ \text{cm}^{-1}$).

We would then tentatively interpret the onset of the PLE spectrum near 0.8 eV as due to the allowed $^4T_1 \rightarrow {}^4T_2$ absorption transition. Figure 10(g) presents the spin-inversion between Cr^{3+} ($^4T_2$) and Cr^{3+} (^2E).

Many authors have reported on the photoconductivity of GaAs:Cr. Eaves *et al.*[28] have even observed the ZPL of the internal transition of Cr^{2+} at 0.820 eV by photoconductivity. The mechanism that was supposed to be involved is

$$Cr^{2+}(^5T_2) + h\nu \rightarrow Cr^{2+}(^5E) \rightarrow Cr^{3+} + e(\text{CB})\ .$$

This mechanism is indeed responsible for photoconductivity. However, as shown in Fig. 10, if that process would only concern a t_2 electron, the system would be left in the excited Cr^{3+} ($^4T_1$) state which is much higher in energy. Therefore, if we want to explain the photoconductivity of GaAs:Cr, some sort of Auger process must be occurring: one electron needs some energy to go from a t_2 orbital to the conduction band, this energy must be given by another electron that goes down to an e orbital (see Fig. 10) and finally the system is left as Cr^{3+} ground state ($^4T_1$) plus one electron in the conduction band.

This Auger effect is possible if the energy gained by one electron when going back to an e orbital is greater than the energy needed to promote an electron from a t_2 orbital to the conduction band. This is actually the case for chromium in GaAs.

III. BAND-SHAPE CALCULATIONS

The main problem in reproducing the band shapes of the optical transitions at Cr^{2+} ions lies in the asymmetry of the emission band compared to the rather symmetric corresponding absorption band.

The first band-shape calculation on Cr^{2+} has been performed by Kaminska *et al.*[58] in II-VI compounds. This calculation is made in the semi-classical approximation by taking into account spin-orbit coupling. In the case of ZnSe:Cr where the spin-orbit coupling is estimated to be negligible, the double-peaked band shape was explained by a small, but not 0, Jahn-Teller effect in the ^5E excited state (see Fig. 4 of Ref. 58).

However, the results of Kaminska *et al.* are based on an unacceptable assumption: They indeed assume different transition probabilities for emission and absorption between the same levels. The transition $^5B_2 \rightarrow {}^5B_1$ is taken as forbidden (as it should) in absorption but allowed in emission. The situation is presented in Fig. 13, where the effect of a Jahn-Teller distortion of the $^5T_2$ state and of the ^5E state is shown in the Q_θ direction.

This assumption, $^5B_2 \rightarrow {}^5B_1$ allowed as well as $^5B_2 \rightarrow {}^5A_1$, allows Kaminska *et al.*[58] to find the double-hump shape for the emission transition. When the correct probabilities are introduced, the observed shape cannot be obtained (see Fig. 14). In the following we summarize the calculations that we have made to find the origin of the band shape.

A. Static Jahn-Teller effect in the ^5E state

In the static case, for the ^5E excited state, the Jahn-Teller Hamiltonian is

$$\mathcal{H}^i_{\text{JT}} = V_2(Q_\theta u_\theta + Q_\epsilon u_\epsilon) + \tfrac{1}{2}k(Q_\theta^2 + Q_\epsilon^2)I$$

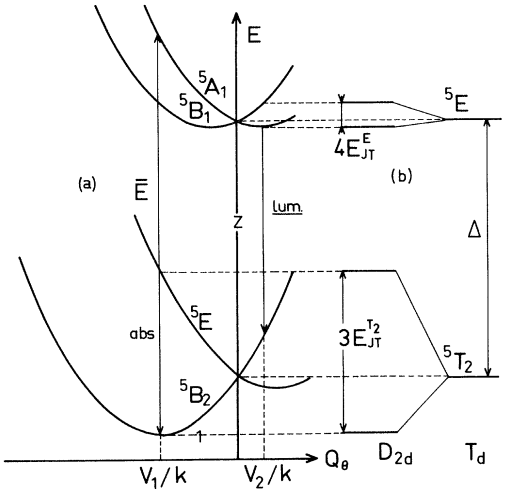

FIG. 13. Scheme showing the effect of Jahn-Teller coupling in the $^5T_2$ and in the ^5E state in the Q_0/E plane.

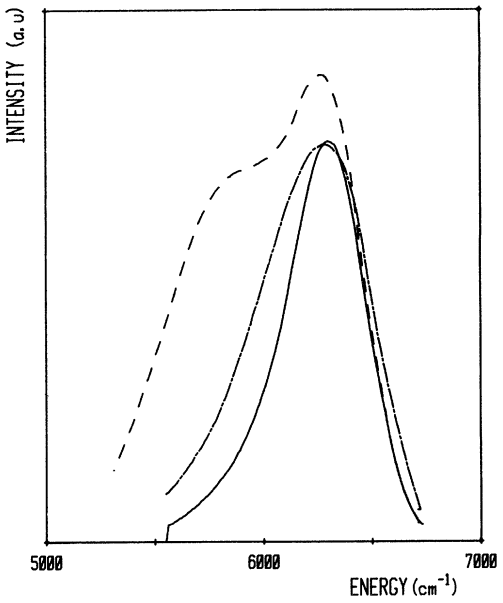

FIG. 14. Band shapes obtained for $^5E \rightarrow {}^5T_2$ emission transition if $E_{JT}(^5E)=50\ cm^{-1}$, $E_{JT}(^5T_2)=600\ cm^{-1}$. (a) Dashed line: Kaminska'a assumption: $^5B_1 \rightarrow {}^5B_2$ transition is allowed (Ref 47); two humps are observed. (b) Solid line: Introduction of the proper transition probabilities in the semiclassical approximation. (c) Dotted-dashed line: The same shape is obtained by performing a vibronic calculation.

where

$$u_\theta=\begin{bmatrix}-1 & 0\\ 0 & 1\end{bmatrix},\quad u_\epsilon=\begin{bmatrix}0 & 1\\ 1 & 0\end{bmatrix},\quad I=\begin{bmatrix}1 & 0\\ 0 & 1\end{bmatrix},$$

and Q_θ, Q_ϵ are normal vibration coordinates of the ϵ mode. In polar coordinates, the eigenvalues and eigenfunctions are

$$E_i^{\pm}=E_0\pm V_2\rho+\tfrac{1}{2}\mu\omega^2\rho^2,$$

$$\psi^+(\rho,\theta)=\begin{bmatrix}\sin\frac{\theta}{2}\\ \cos\frac{\theta}{2}\end{bmatrix},\quad \psi^-(\rho,\theta)=\begin{bmatrix}\cos\frac{\theta}{2}\\ -\sin\frac{\theta}{2}\end{bmatrix},$$

which correspond to the upper and lower branch of the "mexican hat." If the $^5T_2$ state is coupled to the same ϵ mode, we write in the following the same way:

$$\mathscr{H}_{JT}^f=V_1(Q_\theta\xi_\theta+Q_\epsilon\xi_\epsilon)+\tfrac{1}{2}k(Q_\theta^2+Q_\epsilon^2)I$$

where

$$\xi_\theta=\begin{bmatrix}\frac{1}{2} & 0 & 0\\ 0 & \frac{1}{2} & 0\\ 0 & 0 & \frac{1}{2}\end{bmatrix}$$

and

$$\xi_\epsilon=\begin{bmatrix}-\frac{\sqrt{3}}{2} & 0 & 0\\ 0 & \frac{\sqrt{3}}{2} & 0\\ 0 & 0 & 0\end{bmatrix},$$

and

$$E_f=\tfrac{1}{2}\mu\omega^2\left[\left[Q_\theta+\frac{V_1}{k}\cos\varphi\right]^2+\left[Q_\epsilon+\frac{V_1}{k}\sin\varphi\right]^2\right]$$

with $\varphi=\frac{\pi}{3},\pi,\frac{5\pi}{3}$.

The vibronic functions are $\psi_\xi,\psi_\eta,\psi_\zeta$.

The properties of Cr in GaAs are very close to those of Cr^{2+} in ZnSe, so it is *a priori* possible, as assumed in Ref. 29, that the spin-orbit coupling constant of Cr in GaAs be very weak. We have therefore, for obvious reasons of simplicity, carried out the band-shape calculations without spin-orbit coupling. In the semiclassical approximation, the optimal cross section of the luminescence transition is[58]

$$\sigma(h\nu)=\sum_{\alpha=\pm}\sum_{\gamma=\xi,\eta,\zeta}M^2\int\int dQ_\theta dQ_\epsilon\exp\left[-\frac{E_i^\alpha}{k_BT}\right]\times|\langle\psi^\alpha|p|\psi_\gamma\rangle|^2\times\delta(h\nu-E_i^\alpha+E_f^\gamma),$$

where all symbols have their usual meaning. Using Koster-Slater tables[59] it is easy to calculate the relative electronic transition probabilities $|\langle\psi^{\alpha}|p|\psi_{\gamma}\rangle|^2$. For example,

$$|\langle\psi^{-}|p_x|\psi_{\xi}\rangle|^2=\left|\cos\left[\frac{\theta}{2}+\frac{\pi}{3}\right]\right|^2,$$

$$|\langle\psi^{-}|p_y|\psi_{\xi}\rangle|^2=|\langle\psi^{-}|p_z|\psi_{\xi}\rangle|^2=0,$$

etc. (calculations are made as if V_1 and V_2 have the same sign). It can be verified that the transition probabilities towards each of the $^5T_2$ potential wells are equal. Calculations can thus be carried out considering only one well, for example the well ζ, and then multiplying by 3:

$$\sigma(h\nu)=3M^2\left[\int\int dQ_{\theta}dQ_{\epsilon}\cos^2\frac{\theta}{2}\exp\left[-\frac{E_i^-}{k_BT}\right]\delta(h\nu-E_i^-+E_f)\right.$$
$$\left.+\int\int dQ_{\theta}dQ_{\epsilon}\sin^2\frac{\theta}{2}\exp\left[-\frac{E_i^2}{k_BT}\right]\delta(h\nu-E_i^+ +E_f)\right]$$

where

$$E_i^{\pm}-E_f=E_{\mathrm{ZPL}}-V_1\rho\cos\theta+V_2\rho-\frac{V_1^2-V_2^2}{2k}.$$

Integration over θ can be performed by setting

$$\epsilon=h\nu-E_{\mathrm{ZPL}}+\frac{V_1^2-V_2^2}{2k},\quad \cos\theta=-\frac{\epsilon-V_2\rho}{V_1\rho}=\alpha,$$

so that if $\epsilon>0$, $\rho_{\mathrm{inf}}=\epsilon/(V_1-V_2)$; if $\epsilon<0$, $\rho_{\mathrm{inf}}=|\epsilon|/(V_1+V_2)$, and finally

$$\sigma(h\nu)=3M^2\left[\int_{\rho_{\mathrm{inf}}}^{\infty}\frac{V_1\rho-\epsilon+V_2\rho}{2V_1\rho}\exp\left[-\frac{k(\rho+V_2/k)^2}{k_BT}\right]\frac{\rho_d\rho}{[(V_1\rho)^2-(\epsilon-V_2\rho)^2]^{1/2}}\right.$$
$$\left.+\int_{\rho_{\mathrm{inf}}}^{\infty}\frac{V_1\rho+\epsilon+V_2\rho}{2V_1\rho}\exp\left[-\frac{k(\rho-V_2/k)^2}{k_BT}\right]\frac{\rho_d\rho}{[(V_1\rho)^2-(\epsilon+V_2\rho)^2]^{1/2}}\right].$$

The integration can then be carried out easily by a computer. The calculation differs from that of Kaminska *et al.*[47] only by the introduction of the electronic transition probabilities $\cos^2\theta/2$ and $\sin^2\theta/2$. If the calculations of Kaminska *et al.*[58] gave a double-peak shaped band, the introduction of the coefficients $\cos^2\theta/2$ and $\sin^2\theta/2$ suppresses the second band (see Fig. 14). So the shape of the Cr^{2+} emission band cannot be obtained in the semiclassical approximation (double-humped shape) with only the introduction of the ^5E linear Jahn-Teller effect.

B. Dynamic Jahn-Teller effect in the ^5E state

We have then assumed that this difficulty was due to the fact that the dynamic character of the ^5E wave functions was not properly taken into account. In order to check that point we have performed a complete vibronic calculation (not including spin-orbit effects) following Longuet-Higgins *et al.*[60] and Muramatsu.[61]

The vibronic wave functions of the initial state are

$$\psi_{l+}^{p}=\sum_{n=1,2,\ldots}^{\infty}a_{n,l}^{p}\phi^{+}_{|l|-(1/2)+n,|l|-1/2}+\sum_{n=2,4,\ldots}^{\infty}a_{n,l}^{p}\phi^{-}_{|l|-(1/2)+n,|l|+1/2}$$

and

$$\psi_{l-}^{p}=\sum_{n=1,3,\ldots}^{\infty}a_{n,l}^{p}\phi^{-}_{|l|-(1/2)+n,-(|l|-1/2)}+\sum_{n=2,4,\ldots}^{\infty}a_{n,l}^{p}\phi^{+}_{|l|-(1/2)+n,-(|l|+1/2)},$$

where the coefficients $a_{n,l}^{p}$ are solutions of

$$\begin{bmatrix} m_0+1 & k(m_0+1)^{1/2} & \cdots & 0 & \cdots & \cdots \\ k(m_0+1)^{1/2} & m_0+2 & k\sqrt{1} & & & \\ & k\sqrt{1} & m_0+3 & k(m_0+2)^{1/2} & & \\ \cdots & 0 & \cdots & k(m_0+2)^{1/2} & m_0+4 & k\sqrt{2} \end{bmatrix}$$

and $\phi_{n,m}^{\pm}=\psi_{\pm}\chi_{n,m}(\rho,\theta)$ (see Ref. 49), with $m_0=|l|-\frac{1}{2}$. The wave functions of the $^5T_2$ final state are

$$|x\rangle\chi^D_{n,m}\ ,\quad |y\rangle\chi^D_{n,m}\ ,\quad |z\rangle\chi^D_{n,m}\ ,$$

where $\chi^D_{n,m}$ means displaced two-dimensional harmonic oscillator wave functions. Those wave functions are for an oscillator centered on each of the wells, and $\chi_{n,m}$ are the undisplaced harmonic oscillator wave functions.

Following Muramatsu and Sakamoto,[62] we write the vibronic wave functions of the $^5T_2$ state, using the undisplaced harmonic oscillator functions as vibrational base. The vibronic basis is then

$$\phi_n(\Gamma,\gamma)=|\gamma\rangle\sum_{m=n+1}^{n-1}P_{n,m}(\Gamma,\gamma)\chi_{n,m}\ ,$$

where $|\gamma\rangle$ is the electronic part x, y, or z and the $P_{n,m}$ are generated from a recursion relation based on Lanczo's method[63] (see Ref. 61). Finally the $^5T_2$ vibronic wave functions are

$$\psi^q_{n'}(\Gamma,\gamma)=\sum_{n=n'}^{\infty}b^q_{n',n}(\Gamma)\phi_n(\Gamma,\gamma)\ ,$$

where the $b^q_{n',n}$ are solutions of

$$\begin{bmatrix} n'-\epsilon & -\sqrt{S} & & & \\ -\sqrt{S} & n'+1-\epsilon & -\sqrt{2S} & & 0 \\ & -\sqrt{2S} & n'+2-\epsilon & -\sqrt{3S} & \\ & & -\sqrt{3S} & n'+3-\epsilon & -\sqrt{4S}\ \cdots \\ \cdots & 0 & \cdots & \cdots & \cdots \end{bmatrix}$$

with $S=V_1^2/2\mu\omega^2\hbar\omega$ and $\epsilon=q\hbar\omega$. The electronic matrix elements are

$$\langle\psi_\pm|p_x|x\rangle=\pm\exp\left[\pm\frac{2i\pi}{3}\right]\cdots$$

where the ellipsis represents additional elements (see Ref. 62). For symmetry reasons, calculations can be made on the P_z polarization alone, and the band shape can be expressed as

$$W_z=M^2\sum_l\sum_p\sum_{n'}\sum_q|\langle\psi^p_{l\pm}|p_z|\psi^p_{n'}(\Gamma,z)\rangle|^2\exp\left[-\frac{E^e_{l,p}}{k_BT}\right]\delta(E^e_{l,p}-E^f_{n',q})$$

$$=M^2\sum_l\sum_p\sum_{n'}\sum_q\sum_i\sum_j\sum_m a^p_{l,l}b^q_{n',j}P_{j,M}|\langle\pm|p_z|z\rangle|^2|\langle\chi_{|l|+(1/2)+i,|l|+1/2}|\chi_{j,m}\rangle|^2$$
$$\times\exp\left[-\frac{E^e_{l,p}}{k_BT}\right]\delta(E^e_{l,p}-E^f_{n',q})$$

as $|\langle\chi_{n,m}|\chi_{n',m'}\rangle|^2=\delta_{n,n'm,m'}$. The expression can be simplified to

$$W_2=M^2\sum_l\sum_p\sum_{n'}\sum_q\sum_i a^p_{l,l}b^q_{n',|l|-1/2+i}P_{|l|-1/2+i,|l|+1/2}\exp\left[-\frac{E^e_{l,p}}{k_BT}\right]\delta(E^e_{l,p}-E^f_{n',q})\ .$$

Numerical diagonalization of matrices, and calculation of the band shapes has been performed. Results of such a calculation are in very good agreement with those obtained by the semiclassical approach (see Fig. 14).

C. Introduction of spin-orbit effects

Unfortunately, it is not possible to fit the experimental results with the model that we have used. Another parameter must be included. The first one that comes to mind is the spin-orbit coupling that we have neglected; the second one is the coupling to other vibration modes (either ϵ modes of different frequency or τ_2 modes). Semiclassical calculations including spin-orbit effects have been carried out by Kaminska *et al.*[48] with the restrictions that we have raised. However, band-shape calculations using vibronic matrices and including spin-orbit effects need the diagonalization of very large matrices (typically 5000×5000). The calculation of many eigen functions in such a case is very difficult.

As we just showed above, semiclassical calculations cannot be handled if the Jahn-Teller coupling is not 0 in the excited state. If we suppose that the Jahn-Teller effect in the ^5E excited state is almost 0 so that transition occurs near $Q_\theta=Q_\epsilon=0$ for luminescence, we may in a first approximation assume that the transition probabilities are constant near $Q_\theta=Q_\epsilon=0$. It is possible to calculate those probabilities, and we have performed a very simple calculation of the same type as Kaminska *et al.*[58] and Cho.[64] The result is in general a band shape with three peaks. The distance between them is approximately 2λ and 3λ (spin-orbit splitting at $Q_\theta=Q_\epsilon=0$; see Fig. 15). In our case, the band shape shows two humps at a distance of

about 500 or 600 cm^{-1}. That would give a spin-orbit coupling constant close to 100 cm^{-1}, greater than the free-ion value. So unless complete vibronic calculations give a very different result, spin-orbit effects alone cannot explain the band shape that we observe. Furthermore, as shown in Ref. 29 the spin-orbit coupling constant is likely to be reduced by covalency effects and so it can be thought to play only a minor role.

Another possible cause would be the coupling to other vibration modes. Amongst these the case of equal coupling to an ϵ and a τ_2 mode of the same frequency is the most easy to perform. Calculations have been carried out by different authors[64–68] and the results presented by O'Brien *et al.*[65] are in very good agreement with our experimental results [see Fig. 5 in Ref. 54].

EPR absorption and luminescence results (ZPL) are consistent with the description in terms of a $^5T_2$ state only coupled to an ϵ mode. If the state would be equally coupled to one ϵ and one τ_2 vibration mode, the dynamic Jahn-Teller regime would be observed. As this is not so, the V_{τ_i} coupling coefficient is known to be weaker than the V_ϵ coupling coefficient. However, the V_{τ_2} coupling coefficient is not necessarily negligible, since it is quenched near the potential minima and thus not observed in EPR or absorption. Although Picoli *et al.*[11] have assumed the occurrence of a nonzero coupling to τ_2 modes, this effect is seemingly too small to explain the observed band shape.

A less complete calculation, but in a more general case, has been performed by Cho.[64] He calculated the $A_1 \rightarrow T_2$ band shapes if the T_2 state is coupled to A_1, ϵ, and τ_2 vibration modes and subjected to spin-orbit coupling. This case is equivalent to our system if the Jahn-Teller effect would be negligible in the ^5E excited state. Several figures in Ref. 64 correspond quite closely to the band shape that we have observed, but they all need the introduction of a nonnegligible coupling to a τ_2 vibration mode (see Figs. 6, 8, and 12 of Ref. 64).

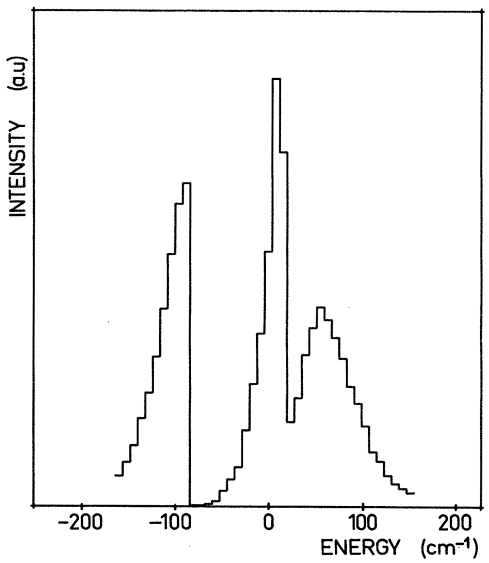

FIG. 15. Band shape in the semiclassical approximation with the following parameters [after Cho (Ref. 53)]. $E_{JT}(^5T_2)=600$ cm^{-1}, $E_{JT}(^5E)=50$ cm^{-1}, $\lambda=50$ cm^{-1}.

D. Quadratic Jahn-Teller effect in the ^5E state

Another possibility that can be examined is the occurrence of a small quadratic Jahn-Teller effect in the ^5E excited state. Such a small effect can change the wave functions of the lower states in a large way. In that case, we use the semiclassical band-shape calculation. The $^5T_2$ state description is unchanged. The new Hamiltonian for the ^5E state is

$$\mathcal{H}_{JT}=\tfrac{1}{2}k(Q_\theta^2+Q_\epsilon^2)I+V_2(Q_\theta u_\theta+Q_\epsilon u_\epsilon)+K_2[(Q_\epsilon^2-Q_\theta^2)u_\theta+2Q_\theta Q_\epsilon u_\epsilon],$$

which gives, for eigenvalues and eigenfunctions,

$$E_i^{\pm}=E_0+\tfrac{1}{2}k\rho^2\pm(V_2^2\rho^2+K_2^2\rho^4-2V_2K_2\rho^3\cos3\theta)^{1/2},$$

$$\psi_i^{\pm}=|+\rangle\cos\alpha^{\pm}+|-\rangle\sin\alpha^{\pm},$$

with

$$\tan\alpha^{\pm}=\frac{-(V_2\rho\cos\theta-K_2\rho^2\cos2\theta)\pm(V_2^2\rho^2+K_2^2\rho^4-2V_2K_2\rho^3\cos3\theta)^{1/2}}{V_2\rho\sin\theta+K_2\rho^2\sin2\theta},$$

and the optical cross section for luminescence is now

$$\sigma(h\nu)=\sum_{\pm}M^2\int\int\rho\,d\rho\frac{l}{1+\tan\alpha^{\pm}}\exp\left[-\frac{1}{k_BT}\left[\rho^2+\frac{V_2^2}{2K}\pm k_2^2\rho^4-2V_2K_2\rho^3\cos3\theta\right]\right]\delta(h\nu-E_i^{\pm}+E_f)d\theta.$$

The introduction of the quadratic coupling term changes the energy only slightly; more affected are the transition probabilities by the change in the ground-state wave functions by the introduction of the $\cos^2\alpha^{\pm}$ term. Owing to the occurrence of the $\rho^3\cos3\theta$ term, exact calculations are very difficult to perform; however, if K_2 is small, the eigenvalue can be approximated by:

$$\lambda^{\pm}=\pm V_2\rho(1-K_2V_2\rho^3\cos3\theta)$$

If V_2 has a sign opposite to V_1, the luminescence band

is displaced towards high energies. The introduction of a K_2 term having the same sign as V_2 brings a low-energy shoulder whose intensity increases with K_2 and with V_2.

A good approximation of the band shape is obtained (see Fig. 16) if $E_{JT}(^5T_2)=600$ cm^{-1}, $E_{JT}(^5E)=50$ cm^{-1}, $K=-0.0025$ in $\hbar\omega$ units ($\hbar\omega=80$ cm^{-1}). Therefore, the double-humped band shape is due to the presence of a small quadratic Jahn-Teller effect. As in ZnSe, spin-orbit effects seem to be negligible in first order. This effect does not influence the absorption curve which mainly involves the high-energy states of the "mexican hat." The quadratic term is 2% of the linear term (-0.125 in $\hbar\omega$ units).

In conclusion, the most probable effect giving rise to the double-humped band shape of the Cr^{2+} internal luminescence is the occurrence of a small quadratic term in the Jahn-Teller coupling of the ^5E excited state. Estimated Jahn-Teller energies are 600 cm^{-1} for the ground state and 50 cm^{-1} for the excited state.

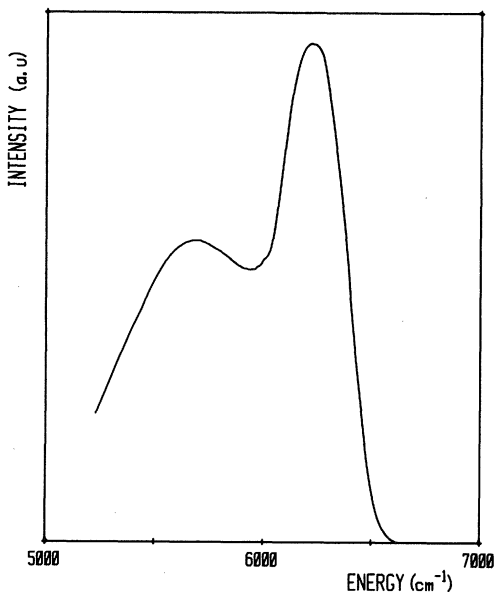

FIG. 16. Effect introduced by a quadratic term in the ^5E excited state: $E_{JT}(^5E)=50$ cm^{-1}, $E_{JT}(^5T_2)=600$ cm^{-1}, quadratic term $K_2=-0.0025$ in $\hbar\omega$ units ($\hbar\omega=80$ cm^{-1}).

CONCLUSIONS

We have used different experimental techniques in order to observe the Cr^{2+} internal transition in GaAs. Under usual conditions, this luminescence is not observed because the ^5E excited state of Cr^{2+} is above the conduction-band minimum. In order to observe this luminescence the first idea is to bring the ^5E level below the conduction band. This has been performed in two ways: applying an hydrostatic pressure or alloying with aluminum. Unfortunately, in these two experiments, the ZPL that would ascertain the attribution of the band to Cr^{2+} cannot be observed. The ZPL has finally been observed in GaAs by using 1.32-μm (0.9-eV) excitation. This zero phonon line is perfectly in agreement with that which was expected, following absorption results. The shape of the internal transition of Cr^{2+} in GaAs is then deduced by a deconvolution procedure and found to agree with what is observed in $Ga_{1-x}Al_xAs$:Cr.

PLE spectra have been recorded in $Ga_{1-x}Al_xAs$ and in GaAs. Apart from the internal transition, these spectra show a drastic increase at the band edge when the luminescence is highly favored ($Ga_{1-x}Al_xAs$). A model in terms of one-electron orbitals is presented to explain the capture process of photoexcited carriers. This model shows that Cr^{2+} internal luminescence is excited by the capture of an electron-hole pair (or of an exciton) at a Cr^{2+} center. The same model is applied to other transition-metal elements in III-V materials and is found to explain experimental observations. This model leads us to explain the 0.57-eV line in p-type GaAs (Cr as an internal transition of Cr^{3+}) and to propose that the photoconductivity is assisted by an Auger effect. Band-shape calculations allow us to show that the double-humped shape of the luminescence is mainly due to the Jahn-Teller effect in the ^5E state with a small nonlinear term.

ACKNOWLEDGMENTS

The authors wish to thank A. M. Hennel, B. Clerjaud, and A. Gelineau for helpful discussions during this work. The technical assistance of H. L'Haridon has been greatly appreciated.

[1]A. M. Huber, G. Morillot, N. T. Linh, P. N. Favennec, B. Deveaud, and B. Toulouse, Appl. Phys. Lett. 34, 858 (1979).

[2]P. N. Favennec and H. L.'Haridon, in *Proceedings of the First Semi-Insulating III-V Materials Conference, Nottingham, 1980,* edited by G. J. Rees (Shiva, Nantwich, 1980), p. 130.

[3]B. Tuck, G. A. Abdegoyega, P. R. Jay, and M. J. Cardwell, in *Proceedings of the GaAs and Related Compounds Conference, St. Louis, 1978,* edited by C. H. Wolfe (IOP, London, 1979), p. 114.

[4]G. Picoli, B. Deveaud, and D. Galland, J. Phys. (Paris) 42, 133 (1981).

[5]A. M. Hennel and G. Martinez, Phys. Rev. B 25, 1039 (1982).

[6]G. H. Stauss and J. J. Krebs, Phys. Rev. B 22, 3141 (1980).

[7]D. C. Look, S. Chaudhuri, and L. Eaves, Phys. Rev. Lett. 49, p. 1728 (1982).

[8]E. C. Lightowlers, M. O. Henry, and C. M. Penchina, in *Proceedings of the 15th Conference on the Physics Semiconductors—Edinburgh,* edited by B. L. H. Wilson (IOP, London, 1978), p. 307.

[9]G. Picoli, B. Deveaud, and D. Galland, in *Proceedings of the First Semi-Insulating III-V Materials Conference, Nottingham, 1980,* edited by G. J. Rees (Shiva, Nantwich, 1980), p. 254.

[10]M. S. Skolnick, M. R. Brozel, and B. Tuck, Solid State Commun. 43, 379 (1982).

[11]G. Picoli, B. Deveaud, B. Lambert, and A. Chomette, J. Phys.

Lett. (Paris) 44, 85 (1983).
[12]B. Deveaud, B. Lambert, G. Picoli, and G. Martinez (to be published in J. Appl. Phys.).
[13]H. Ennen, U. Kaufmann, and J. Schneider, Appl. Phys. Lett. 38, 355 (1981).
[14]B. Deveaud, B. Lambert, and A. M. Hennel, in The Fourth "Lund" Conference, Eger, Hungary, 1983 (unpublished).
[15]U. Kaufmann and J. Schneider, Solid State Commun. 20, 143 (1976).
[16]J. J. Krebs and G. H. Stauss, Phys. Rev. B 16, 971 (1977).
[17]J. J. Krebs and G. H. Stauss, Phys. Rev. B 15, 17 (1977).
[18]J. J. Krebs and G. H. Stauss, Phys. Rev. B 20, 795 (1979).
[19]B. Deveaud, A. M. Hennel, W. Szuszkiewicz, G. Picoli, and G. Martinez, Rev. Phys. Appl. 15, 671 (1980); Second Lund Conference, Ste. Maxime, France, 1979 (unpublished).
[20]A. Nouailhat, F. Litty, S. Loualiche, P. Leyral, and G. Guillot, J. Phys. (Paris) 43, 815 (1982).
[21]G. M. Martin, A. Mitonneau, D. Pons, A. Mircea, and D. W. Woodard, J. Phys. C 13, 3855 (1980).
[22]G. Martinez, A. M. Hennel, W. Szuszkiewicz, M. Balkanski, and B. Clerjaud, Phys. Rev. B 23, 3920 (1981).
[23]A. M. Hennel, W. Szuszkiewicz, M. Balkanski, G. Martinez, and B. Clerjaud, Phys. Rev. B 23, 3933 (1981).
[24]J. T. Vallin, G. A. Slack, S. Roberts, and A. E. Hughes, Phys. Rev. B 2, 4313 (1970).
[25]G. Grebe and H. J. Schultz, Phys. Status Solidi B 54, k69 (1972).
[26]G. Grebe and H. J. Schultz, Z. Naturforsch. 29a, 1803 (1974).
[27]M. Kaminska, J. M. Baranowski, S. N. Uba, and J. T. Vallin, J. Phys. C 12, 2197 (1979).
[28]L. Eaves, P. S. Williams, and Ch. Uihlein, J. Phys. C 14, 1693 (1981).
[29]B. Deveaud, B. Lambert, H. L'Haridon, and G. Picoli, J. Lumin. 24/25, 273 (1981).
[30]B. Deveaud, G. Picoli, Y. Zhou, and G. Martinez, Solid State Commun. 46, 359 (1983).
[31]K. Kocot, R. A. Rao, and G. L. Pearson Phys. Rev. B 19, 1059 (1979).
[32]F. Stern, in *Solid State Physics,* edited by F. Seitz and D. Turnbull (Academic, New York, 1962).
[33]A. S. Abhvani, C. A. Bates, B. Clerjaud, and D. R. Pooler, J. Phys. C. 15, 1345 (1982).
[34]P. J. Williams, L. Eaves, P. E. Simmonds, M. O. Henry, E. L. Lightowlers, and Ch. Uihlein, J. Phys. C 15, 1337 (1982).
[35]B. Clerjaud, A. M. Hennel, and G. Martinez, Solid State Commun. 33, 986 (1980).
[36]J. Barrau, Do Xuan Thanh, M. Brousseau, J. L. Brabant, and F. Voillot, Solid State Commun. 44, 395 (1982).
[37]L. Eaves, T. Englert, C. Uilhein, P. J. Williams, and H. C. Wright, in *Proceedings of the First Semi-Insulating III-V Materials Conference, Nottingham, 1980,* edited by G. J. Rees (Shiva, Nantwich, 1980), p. 145.
[38]F. Voillot, J. Barrau, M. Brousseau, and J. C. Brabant, J. Phys. (Paris) Lett. 41, L415 (1980).
[39]C. Uilhein and L. Eaves, Phys. Rev. B 26, 4473 (1982).
[40]J. Barrau, M. Brousseau, C. A. Bates, and P. Austen, J. Phys. C 16, 4581 (1983).
[41]G. Picoli, B. Deveaud, B. Lambert, and A. Chomette, J. Phys. (Paris) Lett. 44, 185 (1983).
[42]J. Bonnafe, M. Castagne, B. Clerjaud, P. N. Favennec, J. P. Fillard, M. Gauneau, A. Goltzene, B. Guenais, G. Guillot, A. M. Hennel, A. M. Huber, J. Jouglar, P. Leyral, J. C. Manifacier, G. Martinez, G. Picoli, A. Roizesc, C. Schwab, N. Visentin, and P. L. Vuillermoz, Mater. Res. Bull. 16, 1193 (1981).
[43]P. W. Yu, Solid State Commun. 32, 1111 (1979).
[44]F. Voillot, thesis, Université Paul Sabatier, 1981 (unpublished).
[45]T. Instone and L. Eaves, J. Phys. C 11, L771 (1978).
[46]G. M. Martin, A. Mitonneau, D. Pons, A. Mircea, and D. W. Woordard, J. Phys. C. 13, 3855 (1980).
[47]D. J. Robbins and P. J. Dean, Adv. Phys. 27, 499 (1978).
[48]S. G. Bishop, P. J. Dean, P. Porteous, and D. J. Robbins, J. Phys. C 13, 1331 (1980).
[49]D. J. Robbins, J. Lumin. 24-25, 137 (1981).
[50]L. A. Hemstreet and J. O. Dimmock, Phys. Rev. B 20, 1527 (1979).
[51]G. G. De Leo, G. D. Watkins, and W. B. Fowler, Phys. Rev. B 25, 4962 (1982); 25, 4972 (1982).
[52]S. G. Bishop, P. B. Klein, R. L. Henry, and B. D. McCombe, in *Proceedings of the First Conference on Semi-Insulating III-V Materials, Nottingham, 1980,* edited by G. J. Rees (Shiva, Nantwich, 1980), p. 161.
[53]N. Killoran and B. Cavenett, Solid State Commun. 43, 261 (1982).
[54]B. V. Shanabrook, P. B. Klein, and S. G. Bishop, in Proceedings of the 12th International Conference on Defects in Semiconductors Amsterdam, 1983 [Physica 116B, 444 (1983)].
[55]P. E. R. Nordquist, P. B. Klein, S. G. Bishop, and P. G. Siedbenmann, in *Proceedings of the Conference on GaAs and Related Compounds, Vienna, 1980,* edited by H. W. Thim (IOP, London, 1980), p. 569.
[56]M. S. Skolnick, P. J. Dean, P. R. Tapster, D. J. Robbins, B. Cockayne, and W. Mc Ewan, J. Lumin. 24-25, 241 (1981).
[57]U. Kaufmann, M. Ennen, J. Schneider, R. Worner, J. Weber, and F. Kohl, Phys. Rev. B 25, 5598 (1982).
[58]M. Kaminska, J. M. Baranowski, S. M. Uba, and J. J. Vallin, J. Phys. C 12, 2197 (1979).
[59]G. F. Koster, J. O. Dimmock, R. G. Wheeler, and H. Statz, *Properties of the Thirty-Two Point Groups* (MIT Press, Cambridge, 1963).
[60]H. G. Longuet-Higgins, U. Opik, M. H. L. Pryce, and R. A. Sack, Proc. R. Soc. London, Ser. A 244, 1 (1958).
[61]S. Muramatsu, J. Phys. Soc. Jpn. 50, 1645 (1981).
[62]S. Muramatsu, and N. Sakamoto, J. Phys. Soc. Jpn. 46, 1273 (1979).
[63]C. Lanczos, J. Res. Natl. Bur. Stand. (U.S.) 43, 255 (1950).
[64]K. Cho, J. Phys. Soc. Jpn. 25, 1372 (1968).
[65]M. C. M. O'Brien and S. N. Evangelou, J. Phys. C 13, 611 (1980).
[66]M. C. M. O'Brien, J. Phys. C 4, 2524 (1971).
[67]K. Nasu and T. Kosima, Prog. Theor. Phys. 51, 26 (1974).
[68]M. C. M. O'Brien, J. Phys. C 9, 3153 (1976).